Adsorption and Reaction of NO on Ni(100)

Shikong Shen*, P. Feulner, E. Umbach**, W. Wurth, and D. Menzel

Fakultät für Physik E 20, Technische Universität München, Garching bei München, West-Germany

Z. Naturforsch. **42 a,** 1333–1345 (1987); received August 31, 1987

Dedicated to Professor Dr. K. G. Weil on the Occasion of his 60th Birthday

The adsorption, desorption and decomposition of NO on Ni(100) was studied with XPS, UPS, XAES, $\Delta\Phi$, temperature programmed thermal desorption (TPD) and LEED in the temperature range 80 to 1300 K. NO adsorbs molecularly on Ni(100) at low temperatures; dissociation occurs above 200 K. Up to $\approx 1/4$ saturation coverage, only N_2 desorbs in a second order peak around 1100 K. At saturation three NO desorption states at 350, 420 and 1200 K and two N_2 peaks at 660 and 1020 K are observed for a heating rate β of 5 K/s. Activation energies for desorption are obtained by TPD with variable β. Coadsorption experiments show that the NO-TPD peak at 1200 K is due to recombination of N and O on the surface. The relative areas of some TPD maxima depend strongly on coadsorbed O-, C- and N-impurities. At 100 K, $\Delta\Phi$ increases up to a maximum of 1.1 eV at 3/4 saturation coverage and drops to 1.0 eV at saturation. Complex LEED patterns are observed for saturated layers adsorbed below 200 K which change during heating. The nature of the observed binding and desorption states is discussed.

1. Introduction

This study of adsorption, dissociation, desorption and recombination of NO on Ni(100) continues a series of investigations on adsorption of NO on W(110) [1], Ru(001) [2, 3] and Ni(111) [4] by XPS, UPS, XAES, temperature programmed desorption (TPD), work function change ($\Delta\Phi$) and LEED carried out in this laboratory. Besides the practical importance of reactions of NO with transition metals for catalytic processes (see, e.g., [5] and references cited therein), NO adsorption is of fundamental interest because of the possibility to draw parallels to NO coordination complexes, where a good understanding has been established [6]. Furthermore, because of its low atomic number and narrow d-band, Ni is an excellent candidate for quantum chemical calculations and for comparison of theoretical and experimental results [7].

Adsorption of NO on Ni(100) has been investigated before by Onchi and Farnsworth (utilizing LEED and TPD; $T_{ad} = 300$ K) [8], Y. Sakisaka et al. (LEED, AES, ELS, TPD, $\Delta\Phi$ and ESD; $T_{ad} = 300$ K) [9], Price and Baker (LEED, AES, UPS and TPD; $T_{ad} = 85$ K) [10] and Peebles et al. (XPS, UPS, TPD, $\Delta\Phi$, AES and EELS; $T_{ad} = 95$ K) [11]; Stöhr and Jaeger have shown by XANES that molecular NO on Ni(100) at saturation stands upright to within 10 degrees [12]. In particular the work of Peebles et al. is paralleled in some respect by this study. We obtained, however, PES, $\Delta\Phi$ and TPD results which are not contained in [11] and deserve presentation, therefore. Where our results are identical to those of [11], these will be described only briefly, while discrepancies and additional data are presented in more detail. Some data reported here were found to be influenced considerably by contaminants not visible in AES, like carbon dissolved in the bulk which could influence e.g. oxygen concentrations at high sample temperatures by segregating to the surface and giving rise to desorption of oxygen as CO (see below), whereas from perfectly C-depleted Ni(100) crystals only very little CO desorption was found during heating to more than 1000 K after dosing with either NO or O_2 (in these cases the remaining oxygen had to be removed by heating of the sample in hydrogen, see below). All data reported here are from samples being "clean" in the sense that no contaminants were present at the surface during *adsorption* and in temperature ranges where conclusions were drawn from experimental results in question; at higher temperatures, however, influences of reactions as mentioned above will be shown to have happened under some conditions.

* Alexander v. Humboldt Foundation Fellow 1981/83. Permanent address: Lanzhou Institute of Chemical Physics, Chinese Academy of Sciences, PR China.

** New address: 4. Physikalisches Institut, Universität Stuttgart, D-7000 Stuttgart.

Reprint requests to Prof. Dr. D. Menzel, Fakultät für Physik E20, Technische Universität München, D-8046 Garching bei München.

0932-0784 / 87 / 1100-1333 $ 01.30/0. – Please order a reprint rather than making your own copy.

2. Experimental

Experiments were performed on different samples in two different UHV systems. One was equipped for photoelectron spectroscopy (PES), and one for thermal desorption and work function change measurements. For either experiment, single crystal disks of ≈ 1.5 mm thickness and 1 cm^2 area were prepared from a boule supplied by MRC, oriented with a Laue camera to within 0.25 degrees, by spark erosion cutting and mechanical polishing.

2.1 Photoelectron Spectroscopy

XPS, UPS, and XAES data were recorded on two samples in a VG ESCALAB MK I system with a base pressure of 2×10^{-10} mbar, equipped with a 150 deg. spherical analyser, Mg Kα and Al Kα X-ray sources, a He resonance lamp for UPS and 4-grid LEED optics. A microcomputer was used to control the analyser and to collect data. NO from Messer Griesheim (99.85% nominal purity, main impurities N_2, N_2O, CO_2 and NO_2) was dosed by backfilling the chamber with NO. The crystal was mounted between 1 mm thick Ta rods forming a U-shaped spring and fitting in spark cut grooves at its rim. The sample was heated to 500 K by radiation, or close to its melting point by electron bombardment from tungsten filaments suspended in a screening box, which could be moved close to the back of the sample during operation. The crystal could be cooled to 105 K by liquid nitrogen contained in a reservoir which was connected to the sample holder by thick copper braids. Temperature was monitored using a chromel-alumel thermocouple spotwelded to the back of the sample. Further cleaning was done in vacuum by argon sputtering to remove sulphur, and heating/cooling cycles from 500 to 1000 K at heating rates of about 10 K/s in 2×10^{-7} mbar oxygen to remove carbon, followed by annealing to 1300 K. These procedures were repeated until no impurities were visible in XPS, and LEED showed a sharp (1×1) structure (for experiments performed in the second UHV apparatus, the cleaning procedure was slightly changed as indicated in 2.2 below).

2.2 Thermal Desorption and Work Function Changes

The second apparatus (base pressure 3×10^{-11} mbar) was equipped with 4-grid optics for LEED and retard mode AES, an accurate, fast response vibrating capacitor (100 μeV noise at 1 Hz bandwidth, see [13]) for $\Delta\Phi$ measurements, and a quadrupole mass spectrometer (QMS) to record temperature programmed desorption (TPD) spectra. For improved signal to background ratios and exclusion of contributions from crystal rim and holder in TPD, a stagnation tube was added to the ionizer of the QMS as described in [14] in detail. A multiplexer interfaced to the mass spectrometer allowed simultaneous recording of 7 masses and of the sample temperature. Discrimination of gases with equal masses, but different fragmentation behaviour in the ionizer was possible, therefore. For TPD, the sample was mounted between two parallel Ta wires fitting in spark cut grooves at its sides and heated by direct current passage (up to 60 A) through these wires. As for PES, temperatures were measured using a chromel-alumel thermocouple spotwelded to the back of the sample. The sample temperature could either be kept constant within 0.5 K relative to a preset value or varied linearly with time (heating rates $0.1 < \beta < 50$ K/s) by an electronic controller. With the sample used in this experiment, annealing at 1400 K for several minutes was necessary to obtain sharp (1×1) LEED spots. Removal of S and C impurities was done by sputtering and heating in 10^{-6} mbar oxygen for approximately 120 hours as described in 2.1. After this excessive cleaning, however, it was not possible to remove adsorbed oxygen (from dosing either O_2 or NO) by flashing to 1340 K alone (higher temperatures were not used during the measurements to avoid fast degradation of the sample mounting). In these cases, the sample was heated in a hydrogen atmosphere (see 3.2.2; similar cleaning procedures are described in [15]). A microchannelplate gas doser similar to one described in detail before [4, 16] was used to ensure NO purity and sustained low background pressure in the UHV apparatus.

3. Results and Interpretation

3.1 Adsorption

3.1.1 XPS of NO/Ni(100) Adsorbed at 105 K

All XPS spectra shown were recorded using Al Kα radiation; with Mg Kα radiation, Ni LMM

Auger lines interfere with the N1s and O1s binding energy regions. All binding energies are referred to the Fermi level; the latter was determined as described in [4]. The Ni binding energies determined for this surface were identical to those for Ni(111) [4]. NO adsorption at 105 K led to rapid growth of N1s and O1s peaks around 400 eV and 531.5 eV, respectively, see Figure1. The peaks were saturated after $\approx 25 \times 10^{14}$ NO molecules per cm^2 had collided with the surface (i.e. after a dose of 25 Ex [17], where 3.7 Ex correspond to 1 Langmuir for NO at 300 K). As shown in Fig. 1, the peaks shifted monotonically from 400/531.2 eV (N1s/O1s) at low coverages, to 400.2/531.7 eV at saturation, so that the spacing between the two levels increased from 131.2 to 131.5 eV. Similar binding energies have been found for low-temperature adsorption of NO on polycrystalline Ni [18], Ni(111) [4] and Ni(100) [11], and have been interpreted as proof of molecular adsorption; we draw the same conclusion and label this species virgin-NO (v-NO). The BE's given by ref. 11 are slightly different (399.5/531.1 eV at 0.22 monolayers; 400/531.5 eV at 0.55 ML with the spacing staying essentially constant at 131.6 to 131.5 eV). Close inspection of the peak shape, see Fig. 1, reveals an asymmetry of the O1s peak at low coverages (3 – 6 Ex) which would be compatible with a small amount of atomic O (BE $\approx$ 530 eV). The N1s spectra, however, show no trace of atomic N (BE $\approx$ 397 eV), so that a small amount of dissociation (e.g. at steps or other faults) at low coverage appears unlikely. The explanation for the asymmetry is more likely a second, slightly different molecular state (as on Ru(001) [2]), or coadsorption of contaminant from the residual gas in the UHV chamber (a small O1s maximum was always visible on the unexposed sample, see Figure 1). At high coverages (13 – 25 Ex) the O1s peak is seen to broaden considerably from a FWHM of 2.6 eV (13 Ex) to 3.4 eV (25 Ex) with little overall growth, suggesting inequivalent sites in the saturated layer. The intensity ratio of O1s and N1s emission is ~ 1.8, in agreement with the expectation from the transmission function of the spectrometer and from photoionization cross sections [19] for a layer with equal amounts of nitrogen and oxygen.

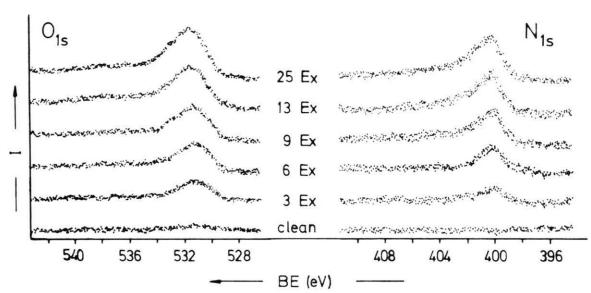

Fig. 1. N1s and O1s XPS spectra for increasing exposures of NO on Ni(100) at 105 K.

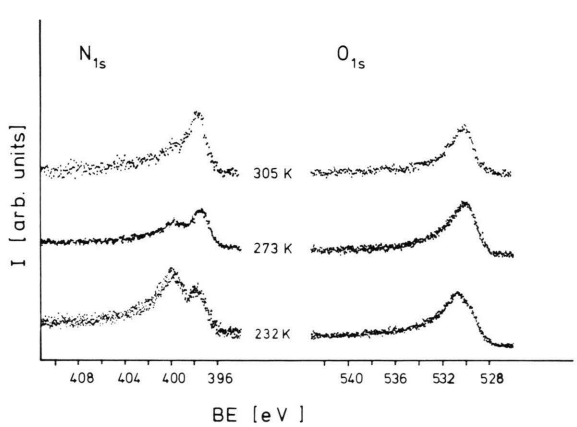

Fig. 2. N1s and O1s regions of saturated (25 Ex) layers of NO on Ni(100) for various adsorption temperatures.

3.1.2 XPS at Adsorption Temperatures between 105 and 305 K

If adsorption was carried out at elevated temperatures, a second N1s maximum at 397.7 eV (3 Ex) to 398.2 eV (25 Ex) BE appeared (Fig. 2), which is indicative of dissociated NO [1, 2, 4, 11]; this species will be labelled β-NO. Relative amounts of v- and β-NO evaluated from N1s peak areas at 400 and 397 eV BE at various adsorption temperatures and for a dosing pressure of 5 to 10×10^{-8} mbar are summarized in Table 1. The v/β-NO ratios are likely to be determined by competition of adsorption with subsequent blocking of sites necessary for dissociation, and dissociation itself. Similar reactions have been observed for other systems [2, 3]

T_{ad} (K)	$\Theta_{v\text{-NO}}$	$\Theta_{\beta\text{-NO}}$
105	1	0
232	0.65	0.35
273	0.4	0.6
305	0.2	0.8

Table 1. Relative quantities of molecularly (v-NO) and dissociatively (β-NO) adsorbed NO/Ni(100) for different adsorption temperatures (adsorption pressure 5 to 10×10^{-8} mbar).

(see however details described in Section 4). At some or all temperatures this ratio could then depend on dosing pressure; this possibility has not been checked, however. At saturation, the O1s peak shifts from 531.7 eV at 105 K, where only v-NO is present on the surface, to 530.3 eV at 305 K, where most NO adsorbs dissociatively.

3.1.3 XPS Satellites, XAES and UPS

N1s and O1s satellites nearly identical to those observed for NO/Ni(111) [4] were obtained. The origin of these satellites has been discussed in detail elsewhere [20]. O-KLL Auger spectra induced by Mg Kα radiation (with Al Kα, Ni2p emission would interfere with the O-KLL lines) were taken for pure v-NO layers ($T_{ad} = 105$ K) and almost pure β-NO layers ($T_{ad} = 335$ K). The v-NO spectra were slightly different from the corresponding ones on Ni(111) [4] and Ru(001) [2], probably due to different collection angles; they correspond clearly to a molecular species, while β-NO is dissociated, see Figure 3. As for NO on Ni(111), molecular Auger energies were found to be shifted by 21 eV relative to the gas phase values, indicating strong screening of the two final state holes in the adsorbate [21].

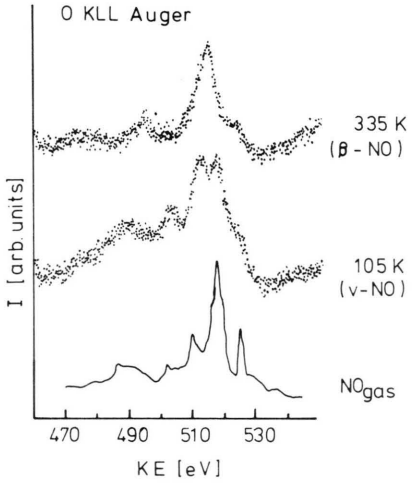

Fig. 3. X-ray induced O KLL Auger spectra for molecular and mainly dissociated NO on Ni(100) (upper two traces), compared to the gas phase NO spectra from Moddeman et al. [21] (the energy scale of the gas phase spectrum is shifted by 21 eV, see text).

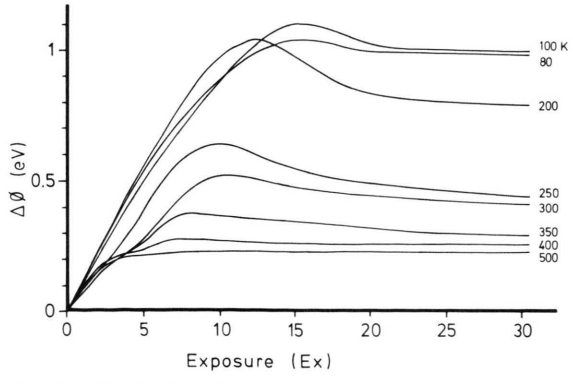

Fig. 4. Work function change during adsorption vs. exposure at different adsorption temperature for pressures of 5 to 10×10^{-8} mbar NO.

He II UPS data obtained from saturated layers ($T_{ad} = 105$ K) were in good agreement with results from ref. 11 and are therefore not shown. Adsorption-induced maxima observed at 14.6 and 8.8 eV are assigned to 4σ, and $5\sigma/1\pi$ emission; decreased intensity in the range of the Ni d-band and of the Ni satellite at 6 eV were observed after adsorption at 105 K.

These XPS satellite, XAES and UPS results corroborate our assignments and those given in [11] of observed photoelectron peaks to molecularly and dissociatively adsorbed NO.

3.1.4 Work Function Changes

Work function changes ($\Delta\Phi$) during adsorption at dosing pressures from 5 to 10×10^{-8} mbar at various temperatures are shown in Figure 4. At 80 and 100 K, where NO is adsorbed only molecularly, Φ increases monotonically with exposure up to 15 Ex, goes through a maximum of 1.02 eV (80 K) or 1.1 eV (100 K) and reaches its saturation value of ≈ 1.0 eV at more than 25 Ex. Similar $\Delta\Phi$ vs. exposure curves are known from layers in which depolarization of the adsorbate molecules takes place during filling of the layer. On the basis of a simple electrostatic model [22] one would expect the extremum of $\Delta\Phi$ closer to zero coverage than to saturation, whereas the opposite is observed here. XPS and TPD data from this work and from [11] show that adsorption is nearly completed (3/4 of saturation) at the maximum of Φ. Other explanations (multi-site binding states with different dipole moments, one binding state which is modified by adsorbate-adsorbate interaction with increasing coverage) come to mind in connection with the XPS peak

asymmetries pointed out above and will be discussed below. The slight curvature of the ascending branch of the curve could point to such processes; it should not be overinterpreted, however, because for reactive gases like NO delayed pressure reading due to adsorption on the walls of the chamber near the ion gauge could lead to an underestimate of the initial doses. If adsorption was carried out at 500 K, $\Delta\Phi$ increased monotonically with dose and reached its saturation value of 0.2 eV at less than 5 Ex. According to the XPS results in Sect. 3.1.2, this curve represents adsorption of pure β-NO. In the intermediate regime, competition between molecular adsorption and dissociation takes place, leading to rather complicated $\Delta\Phi$ traces for these temperatures as shown in Figure 4. As already pointed out, different curves can be expected for different dosing pressures.

While no detailed evaluation of the coverage vs. exposure behaviour has been made, it is clear from the data of Fig. 4 that the sticking coefficient at low temperatures (100 – 200 K) is high (above 0.5) and roughly constant over a considerable coverage range. The high sticking coefficient is also obvious from the data of Figure 1.

In [11], $\Delta\Phi$ data are given only for one adsorption temperature (95 K). The observed shape is similar to ours at 80 – 100 K. The $\Delta\Phi$ values reported for the extremum (0.78 eV/6 Ex) and for saturation (0.73 eV/15 Ex) are different from our values, however. In preliminary studies of CO/Ni(100) we found a maximum $\Delta\Phi$ of 1.3 eV using our Kelvin probe; with the method used in [11] and probably a similar set-up, 1.09 eV were reported for this system [23]. The deviations are of the same order of magnitude for CO and NO and appear to be due to differences in methods. Indeed, different quantities are measured with a vibrating capacitor and, e.g., the onset of the emission of secondary electrons, for a patchy surface. The first method gives an average of the work function, whereas the latter probes its local minima. We believe our method to give a better representation of the intrinsic behaviour of the system.

3.2 Dissociation, Desorption and Recombination of NO During Heating

3.2.1 XPS and UPS

In Figure 5, N1s and O1s spectra are shown as obtained from saturated layers, adsorbed at 105 K, heated to various temperatures, and cooled rapidly before measurement. Amounts of NO molecules and N and O atoms present on the surface at different temperatures were extracted from peak areas of such XPS spectra for different initial coverages (35 and 100% of saturation) and are summarized in Figure 6. Dissociation (or desorption) starts slightly above 200 K for the saturated layer and somewhat lower for the dilute one, and is complete by 400 K, in agreement with results from [11]. The N1s peak decreases between 711 and 875 K (no XPS data are given in [11] for this temperature range) due to de-

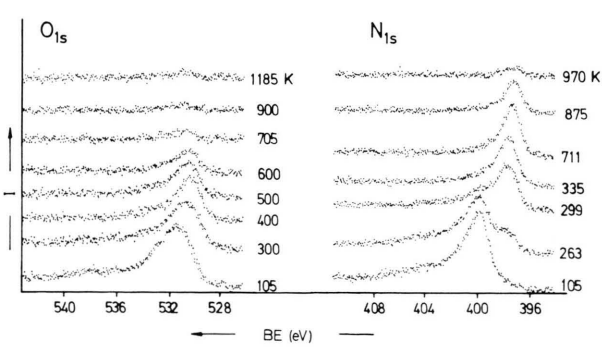

Fig. 5. N1s and O1s regions for saturated layers of NO/Ni(100), prepared by adsorption at 105 K, heating to the indicated temperatures, and cooling before measurement.

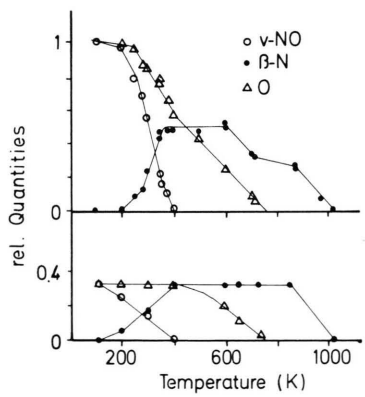

Fig. 6. Relative amounts of NO molecules, and N and O atoms present on the surface after heating of saturated (upper part) and dilute layers (lower part) of NO/Ni(100) to various temperatures (derived from the peak areas of spectra such as those of Figure 5).

sorption of nitrogen (see below), but even at 970 K some nitrogen remains present on the surface. The O1s intensity vs. temperature shows a similar evolution. A signal decrease, however, was also observed between 400 and 700 K, i.e. in a temperature range where no desorption of NO or O_2 occurs (see 3.2.2), and only traces of oxygen are left after heating the sample to 1185 K, see Figure 5. This could be due to diffusion of oxygen into the bulk, as has been observed for NO/Ni(111) [4] and for O/Ni(100) [24]. In [11], however, oxygen was found to stay on the surface up to 1100 K; the residual O-Auger signal at that temperature was used to obtain quantities of dissociated NO. As already mentioned, TPD performed in this work always showed some CO desorption in this temperature range, if the sample had not been heated excessively in oxygen to remove all carbon impurities. If this prolonged cleaning was performed, some oxygen was detectable by electron-induced AES and by LEED (leading to a weak p(2×2) superstructure) after heating the sample to 1200 K as in [11]. This oxygen, which could neither be desorbed, nor diffused into the crystal by further heating to 1400 K, was then removed by heating the sample in 10^{-5} mbar hydrogen at 1200 K for 30 seconds as described in [15]. Such excessive cleaning had not been carried out for those of the present experiments done *before* the TPD experiments, so that some carbon could have diffused to the surface during heating and recombined with O, effectively reducing its coverage. We reiterate that these findings have only minor influences on our PES results, because XPS showed clearly that no C-contaminants were present on the surface under *ad*sorption conditions.

The UPS molecular peaks reported in 3.1.3 vanished after heating to 335 K, and a broad maximum at 5.7 eV, assigned to emission from O2p and N2p, appeared and remained present up to 1040 K. XPS and UPS results from this work and from [11] show clearly that even for saturated layers of NO/Ni(100) heating to 400 K removes all molecular NO.

3.2.2 TPD and $\Delta\Phi$ During Desorption

The QMS signals releated to the masses 12, 14, 28, 30, 44 and 46 and the sample temperature were recorded simultaneously vs. time during each TPD run. Because of the notorious difficulties for quantitative measurements of NO partial pressures [3], no efforts were made to calibrate the sensitivity of the QMS for NO and N_2 in the gas phase to get relative amounts of these desorbing species. For the data shown in Figure 8, however, N_2 and NO scales were adjusted for continuity of the sticking coefficient at 5 Ex, i.e. the dose, for which the onset of molecular NO desorption is obtained (see below for details). Compared to the N_2 signal, the raw NO data shown in Fig. 7a had to be increased by a factor of 4.8. After excessive cleaning of the sample in oxygen, only traces of CO (monitored by mass 12) were detected during TPD, mainly above 1000 K. These CO contributions have been subtracted from

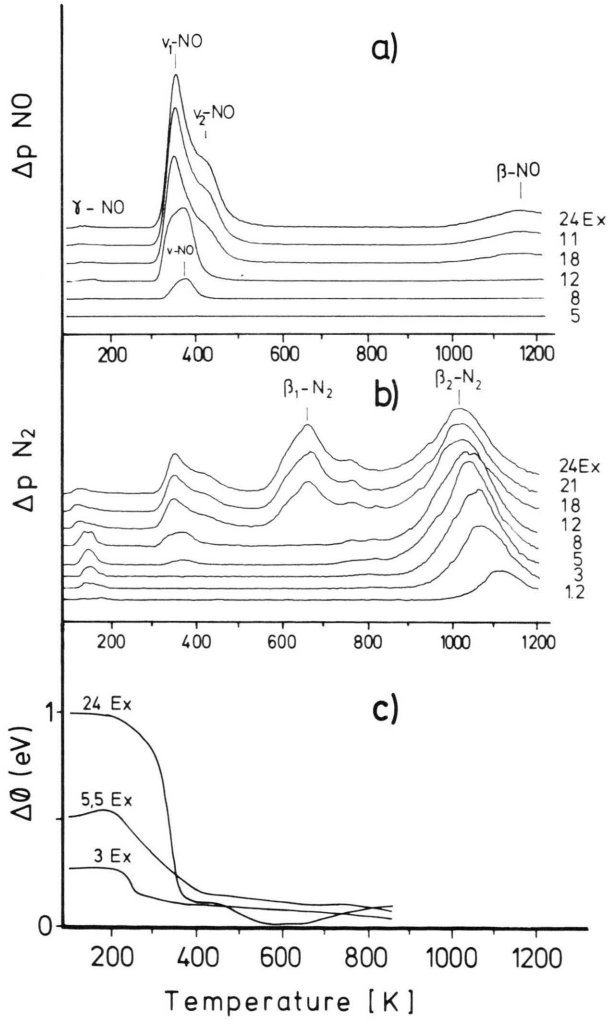

Fig. 7. TPD spectra of (a) NO and (b) N_2, and (c) $\Delta\Phi$, vs. sample temperature for different initial coverages of NO/Ni(100) (heating rate $\beta = 5$ K/s).

all N_2-TPD spectra shown below. No desorption of N_2O or NO_2 was ever found. Small mass 16 signals always paralleling the NO maxima and less than 1% in area of these were obtained. They are interpreted as arising from NO fragmentation in the ionizer of the QMS.

TPD spectra of NO and N_2 recorded at a heating rate $\beta = 5$ K/s from NO/Ni(100) are shown in Figs. 7a,b; the dependence of their peak areas on exposure is summarized in Fig. 8. Small amounts of N_2 and NO desorbed below 200 K (labelled γ). They probably stem from defect sites; desorption from an intrinsic low energy binding state, like for NO/Pt(111) [25], can be excluded, because less than 3% of the total amount desorbed in this temperature range. Below 5 Ex exposure, no NO molecules desorbed. Only the β_2-N_2 maximum was present; the shift of its peak temperature from 1110 K at 1.2 Ex to 1050 K at 5 Ex is compatible with second order desorption. This maximum saturated at 8 Ex; further exposure did not enlarge its area (Figure 8). From 5 to 8 Ex, one v-NO peak grows in at 370 K; its peak temperature does not depend on coverage. When the initial coverage is increased, this maximum exhibits a low temperature shoulder which evolves to the v_1-peak at 350 K with increasing dose. Above 8 Ex, a second NO desorption state (v_2-NO) appears at 420 K, as well as the β_1-N_2 state at 660 K. Further dosing enlarged these maxima; saturation occured at 25 Ex. No shifts of their peak temperatures were observed (the peak temperature of the β_2-N_2 maximum continued to shift from 1050 K to 1020 K in this coverage regime). Comparison of the XPS and TPD results (Figs. 1, 5 and 7a, b) leads to different N1s BE's for pure β_2-layers (397.7 eV) and layers from which β_1-N_2 and v_2-NO TPD maxima were observed (398.2 eV). Neither energy shifts nor new maxima were observed in XPS at exposures related to the onset of molecular NO desorption (v-NO in Figure 7a).

The NO TPD peaks between 350 and 450 K were always accompanied by N_2 peaks of identical shape and $\approx$ 20% in area. Contributions from CO desorption or formation in the ion source of the QMS could be excluded from analysis of the cracking patterns. Cracking of NO and formation of N_2 in electron impact ionizers is usually obtained, as also evident by the lower NO detection efficiency. We therefore do not regard these N_2 maxima parallel to the NO maxima as being of intrinsic nature.

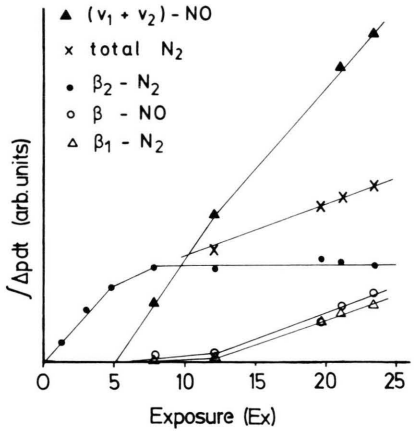

Fig. 8. TPD peak areas from Figs. 7a and 7b vs. exposure. NO and N_2 scales were adjusted for continuity of the sticking probability at the onset of NO desorption (see text). The indicated lines are meant to guide the eye and do not represent an exact dependence.

At saturation, recombination of NO from atomically adsorbed N and O gave rise to an additional NO peak (labelled β-NO) above 1100 K. This feature will be discussed in detail in Section 3.3 below.

One major discrepancy between this work and [10] and [11] is their report of a third nitrogen TPD maximum around 775 K. We found indications of such a peak in this temperature regime (see Fig. 7b), but it was very small. We believe that this maximum is due to residual atomic nitrogen adsorbed on the sample before dosing of NO layers at low temperatures. TPD spectra of [10] and [11] are ending at 1050 K, making it likely that the samples were not heated much higher (we know from our results that N desorption ranges up to 1300 K, see 3.3). This hypothesis is strengthened by the fact that the peak temperature of the β_2-N_2 maximum at low coverage was found to lie considerably lower (1000 K in [11]) than here (1110 K). We mention that (111)-oriented parts of the sample or its edges could also give rise to a TPD peak at this temperature [26]. Comparing the areas of the v_1-NO and v_2-NO TPD maxima obtained in [11] and in this work, one finds that the v_1-NO maximum at 350 K is more pronounced in our spectra than in those of [11]. Coadsorption experiments (see 3.3 below) clearly show that this maximum is strongly attenuated by small amounts of coadsorbed oxygen and we interpret the observed discrepancies as due to coadsorbed oxygen in the work of [11] (even the

data shown in Fig. 7 may have been influenced slightly by coadsorbed oxygen; in a later stage of this investigation, when we had learned to remove the oxygen more reliably from the surface by hydrogen treatment as indicated above, we obtained an even higher ratio of v_1-NO to v_2-NO, see Section 4).

Figure 7c shows $\Delta\Phi$ traces obtained during TPD with $\beta = 5$ K/s for three different initial exposures of NO at 100 K. Up to 200 K a small increase of 50 meV, paralleling the γ-N_2 desorption, was obtained for 5.6 Ex. For exposures of less than 5 Ex (where no desorption of NO molecules was observed) heating above 200 K decreased $\Delta\Phi$. This is interpreted as due to dissociation of NO on the surface, in agreement with the XPS results above. The temperature at which dissociation was complete depended on the initial dose, e.g. 250 K for 3 Ex but 400 K for 5.6 Ex (see Figure 6). At saturation coverage, $\Delta\Phi$ vs. temperature did not change its slope before the onset of the v_1-NO desorption at $\approx$ 350 K; during v_1 desorption, a decrease of 0.7 eV was observed, whereas the work function stayed nearly constant during the desorption of the v_2-state (decrease of less than 50 meV). A further drop of 0.1 eV between 460 K and 560 K followed by an increase above 560 K is probably due to formation of β_1-N_2 and its subsequent desorption. v_1- and v-NO contribute most to the work function change, therefore. For all exposures, some dissociation was found to precede desorption.

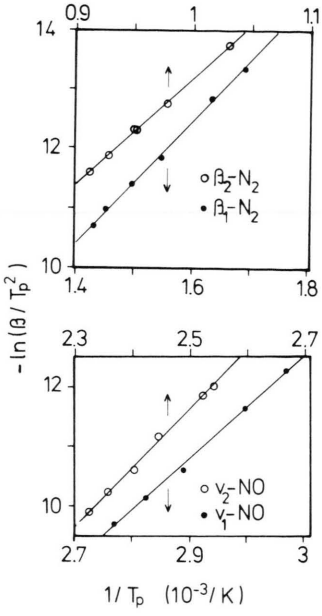

Fig. 9. Evaluation of TPD data taken with variable heating rates according to [27].

Table 2. Peak temperatures (heating rate = 5 K/s) and activation energies for desorption for NO and N_2-TPD states obtained from saturated NO layers on Ni(100) ($T_{ad} = 100$ K).

TPD-state	T_{peak}	E_d (kJ/mole)
v_1-NO	350	72 ± 4
v_2-NO	420	83 ± 4
β_1-N_2	660	90 ± 4
β_2-N_2	1020	152 ± 4

3.2.3 Activation Energies for Desorption

For initially saturated layers, TPD spectra were recorded with different heating rates from 0.5 to 11 K/s. Activation energies for desorption were obtained from TPD peak temperatures according to the method given in [27]. Plotting $-\ln(\beta/T_p^2)$ vs. $1/T_p$ results in straight lines, see Fig. 9, as expected; activation energies for desorption are obtained by dividing the slopes of the lines from Fig. 9 by the Boltzmann number [27]. These energies and the peak temperatures for $\beta = 5$ K/s are summarised in Table 2 for the v_1-NO, v_2-NO, β_1-N_2 and β_2-N_2 TPD states.

3.2.4 LEED

Complex LEED superstructures, changing during heating of the sample, were found for saturated NO layers at $\sim$ 100 K. This is in contradiction to the results of [10], where only an increased background intensity, but no superstructures were found for this coverage regime. After adsorption of a saturated layer of NO at 95 K and heating to 200 K a superstructure of $(4\sqrt{2} \times 4\sqrt{2})$ R 45° symmetry was observed which changed to (6×6) symmetry after further heating to 250 K. For both patterns, some spots were missing. These structures were not investigated in detail; therefore we refrain from further interpretation. Heating to 350 K, which corresponds to the peak temperature of the v_1-NO state, led to a $c(2 \times 2)$ superstructure, which transformed into a $p(2 \times 2)$ pattern after the desorption of the β_1-N_2-state at 700 K. A faint $p(2 \times 2)$ superstructure probably due to oxygen remained visible after the desorption of the β_2-N_2-state up to 1200 K.

3.3 Coadsorption of NO with Oxygen and Nitrogen on Ni(100)

To elucidate the nature of the observed binding and desorption states, especially of the NO-states, preadsorption experiments with atomically adsorbed oxygen and nitrogen were performed on Ni(100). Oxygen was dosed on to the sample with the MCP gas doser at room temperature. Figure 10 shows TPD spectra from saturated, pure NO layers and saturated NO layers dosed on Ni precovered with different amounts of oxygen. The v_1-maximum of the pure layer is slightly enhanced compared to the spectra shown in Figure 7a. The reason for this is that the layers which were used for the experiments presented in 3.2 contained traces of residual oxygen at adsorption conditions. This is obvious from the results shown in Fig. 10: preadsorption of oxygen decreases the height of the v_1-NO TPD peak; it has nearly disappeared at an oxygen does of 7.4 Ex. The other NO-TPD maxima and the β_1-N_2 peak are increased, however. The area of the β_2-N_2 peak is slightly decreased and its peak temperature is shifted to 1010 K.

Preadsorption of atomic nitrogen was produced by bombarding the sample at 85 K with 15 mC/cm^2 of 1000 eV electrons in 5×10^{-7} mbar of nitrogen (a similar procedure was used in [28] to study the adsorption of nitrogen atoms on Ru(001)). From these layers, TPD spectra with maxima at 360 K and 1100 K were obtained, see Figure 11a. The peak at 1100 K probably arose from a β_2-N_2 like species; the higher peak temperature compared to that from NO layers indicates destabilisation of the N–Ni bond by neighbouring oxygen in the latter. Below 200 K, weakly bound nitrogen (probably molecularly adsorbed) desorbed. No NO was observed in TPD (NO could have formed from N and residual oxygen). This shows that we were working with a really oxygen free sample. TPD traces obtained from such a nitrogen layer, heated to 850 K (which removed the nitrogen desorbing in the TPD-state at 360 K), cooled to 100 K and saturated with oxygen are shown in Figure 11b. A nitrogen peak at 1045 K and a NO peak around 1200 K were observed. These peaks are very similar to the β_2-N_2 and the β-NO maxima, respectively, obtained from NO dosed on pure Ni(100) (Figure 7). This shows clearly that the β-NO maximum arises from recombination of adsorbed N and O atoms. The way of preparing this mixed layer (either dissociation of NO or coadsorption of N and O) obviously has negligible influence on the formation of molecular NO at 1200 K, probably because of high mobility of the N and O atoms at these elevated temperatures. The desorption temperature of β-NO must be its formation temperature, as molecular NO would desorb at much lower temperatures (see above).

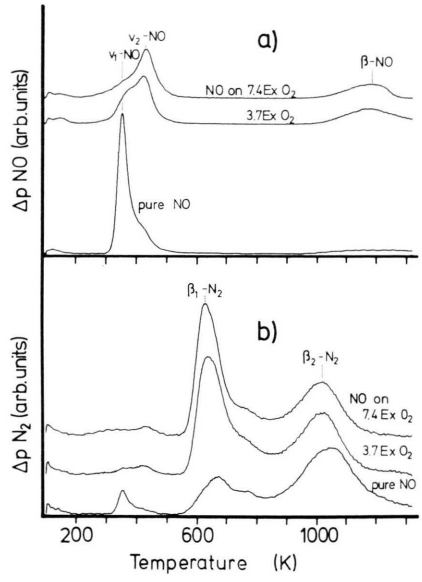

Fig.10. TPD traces of (a) NO and (b) N_2 obtained for saturated NO layers (T_{ad} = 100 K, β = 5 K/s) on Ni(100) preexposed to different doses of oxygen as indicated.

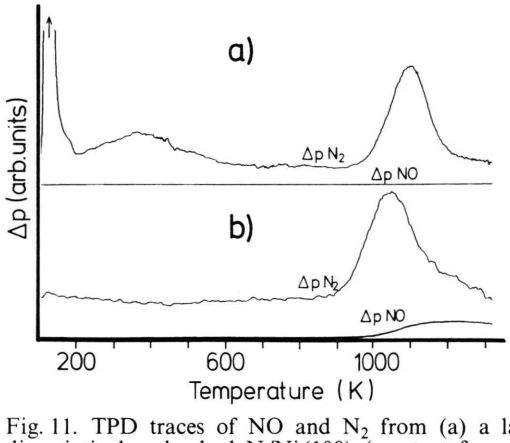

Fig. 11. TPD traces of NO and N_2 from (a) a layer of dissociatively adsorbed N/Ni(100) (see text for preparation) and (b) from such a layer, heated to 850 K and dosed with oxygen to saturation at 100 K.

4. Discussion

As for NO/Ni(111), molecular adsorption of NO occurs at low temperature on Ni(100). In dilute layers of NO, threshold temperatures for dissociation are 300 K and 200 K for Ni(111) [4] and Ni(100), respectively, indicating a higher activity of the latter surface. Dissociation of NO on Ni(100) and Ni(111) is not activated overall (i.e. relative to the gas phase) because dissociation occurs at lower temperatures than desorption. The reason that dissociation does not occur at low temperatures must be due to an activation barrier between molecular and dissociated adsorbate which, however, is below zero (for illustration, see Figure 12b). At low temperatures molecules will then be trapped in the molecular state as observed. At intermediate temperatures, competition between dissociation and molecular desorption is seen to occur. Because of the energetics indicated the exponential in the respective rates is smaller for desorption. As desorption is certainly unhindered entropically, while dissociation can easily contain considerable configurational constraints, the preexponential for desorption should be larger than that for dissociation. As long as available sites are not important for dissociation, we will then expect that dissociation wins the competition in the lower and desorption in the higher temperature range – as observed here. This contrasts somewhat the results on Ru(001) and Ni(111) where site blocking has been observed to be important for coverages close to saturation [2, 3, 4]; this effect is much weaker here, although a shift of dissociation to somewhat higher temperatures is also obtained. We observe dissociation for temperatures above 200 K for dilute and 250 K for saturated layers (in [11], a threshold temperature for dissociation of 295 K is obtained for saturated layers; we mention however that N 1s data in [11] measured after heating a saturated layer of NO to 245 K show a small low BE shoulder which can be attributed to dissociated NO). This may mean that the atomic sites are *not* identical to the molecular ones in the present case. The remaining shift of dissociation temperature may then stem from the necessity of some reordering of the layer at higher coverages.

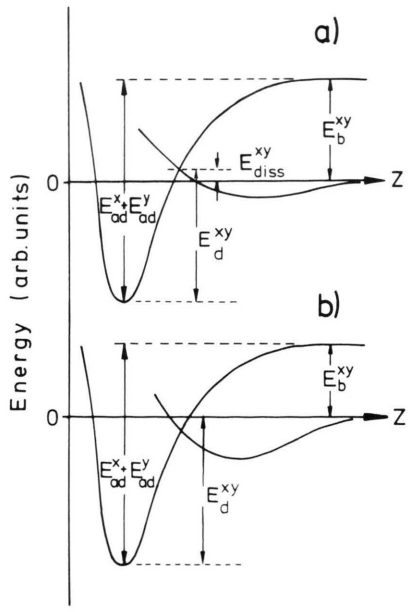

Fig. 12. Definitions of energies used in (1)–(7), and illustration of the situation for (a) activated dissociation as for N_2/Ni(100), and (b) non-activated dissociation competitive with molecular desorption, as for NO/Ni(100).

The similarity of the β_2-N_2 TPD peaks for mixed (N + O) and pure N-layers and the blocking of β_2-N_2 desorption by preadsorption of oxygen (see 3.3) indicate similar adsorption sites for O and N atoms up to a relative coverage of 0.5 for these atoms (corresponding to $\Theta_{NO} = 0.25$), with only weak mutual interaction of both species. As shown, no desorption of intrinsic molecular NO is observed for this coverage regime in agreement with [11].

An observation which has not been reported previously for any other NO adsorption system is the occurrence of a recombinative NO desorption peak at very high temperatures. β-NO is formed from N and O atomically adsorbed on Ni(100) above 1100 K. Recombination of NO from dissociated layers, leading to TD of NO molecules, is observed at 400–600 K for a variety of substrates, so for NO/Ir(100) (1 × 1) [30] and for NO/Ir(110) [31], where NO desorption in two TPD peaks close together at temperatures similar to those observed here for v_1 and v_2-NO was obtained; in both cases, it was shown from isotope exchange experiments that the peaks at higher temperature were at least partially due to recombination of O and N atoms to NO molecules at the surface. Similar conclusions have been drawn for NO adsorbed on defect sites on Pt(111) [32], where NO dissociates on that

surface [25] and for NO on Rh(100) [33]. In these cases, however, recombinative NO desorption is obtained from nearly saturated layers, whereas here β-NO is formed from O and N atoms in dilute layers. Assuming recombinative desorption for N_2 and NO from N and O atoms, desorption rates for nitrogen either as N_2 or as NO can be written as

$$R(N_2) = (-\mathrm{d}\Theta_N/\mathrm{d}t)/2 = k_0\,\Theta_N^2 \exp(-E_d(N_2)/kT), \quad (1)$$

$$R(NO) = (-\mathrm{d}\Theta_N/\mathrm{d}t) = k_0\,\Theta_N\,\Theta_O \exp(-E_d(NO)/kT). \quad (2)$$

k_0, Θ_N, Θ_O, $E_d(NO)$, $E_d(N_2)$ are the prefactor (which should be the same for both cases if fully mobile layers are assumed), the nitrogen coverage, the oxygen coverage, and the activation energies for desorption either as NO or as N_2, respectively. These activation energies depend on the binding energy for the atomic species on the surface, E_{ad}, the heat of dissociation for the desorbing molecule, E_b, and on the activation energy for dissociation of the molecule on the surface, E_{diss}, see Fig. 12:

$$E_d(N_2) = 2x\,E_{ad}^N - E_b^{N_2} + E_{diss}^{N_2}, \quad (3)$$

$$E_d(NO) = E_{ad}^N + E_{ad}^O - E_b^{NO}. \quad (4)$$

The overall activation energy for dissociation of NO is set to zero, see above, so that the activation energy of desorption from the atomic NO state is equal to its adsorption energy. The ratio for desorption of either N_2 or NO is then

$$R(NO)/R(N_2) = (\Theta_O/\Theta_N) \exp((E_d(N_2) - E_d(NO))/kT), \quad (5)$$

where

$$E_d(N_2) - E_d(NO) = E_{ad}^N - E_{ad}^O + E_b^{NO} - E_b^{N_2} + E_{diss}^{N_2}. \quad (6)$$

If the activation energies for both pathways were equal, desorption of NO would dominate for low nitrogen concentration distributed in a high oxygen concentration, because of the term Θ_O/Θ_N in (5). Close inspection of the TD traces in Fig. 7, 10 and 11 clearly reveals that β-NO formation is observed only at the high temperature tail of the β_2-N_2 peak (which is more pronounced for the mixed than the pure N-layer, see Figs. 11 a and 11 b, indicating additional stabilization and/or demobilization of small amounts of nitrogen in an O-layer on Ni(100)), and that excess oxygen increases the rate of NO formation even further. A constant β-NO TPD peak temperature is observed as expected from (2), which shows that the desorption rate of this species is first order in Θ_N. A rough estimate of the difference of the activation energies (3) and (4) for both desorption channels can be based on the Θ_O/Θ_N ratio for the temperature at which equal NO and N_2 desorption rates occur. From our TPD data, we obtain equal desorption rates at 1200 K, where $\Theta_O/\Theta_N \approx 12.5$. By insertion of these values into (5) a difference of the activation energies (6) of $\approx$ 18 kJ/mole is found. With the E_b-values for N_2 and NO from [34], we get a correlation for the adsorption energies of O and N on Ni(100) and the activation energy for dissociation of N_2 on this surface:

$$E_{ad}^O - E_{ad}^N + E_{diss}^{N_2} = 302 \text{ kJ/mole}. \quad (7)$$

Unfortunately, the separate values cannot be obtained. The large difference of the results of (6) and (7) shows that compensation of different terms must be involved; the occurrence of a similar reaction channel for a different substrate seems unlikely.

For higher coverages, two NO- and one additional N_2-TPD peaks were obtained which will be considered next. In [10] and [11], three N_2-TPD maxima and generally lower peak temperatures were obtained which we believe to be caused by coadsorbed N residues as described above. XPS data taken during TPD clearly indicate that NO giving rise to desorption of either v or v_1-NO is molecularly bound; v_1 is the main desorption state obtained for oxygen-free samples, see 3.3. No changes in PES or $\Delta\Phi$ are observed at 105 K for the NO coverage corresponding to the transition from v-NO to v_1-NO in TPD. A similar behaviour was also observed for NO/Ru(001) and is probably due to minor interactional changes of the bonding mode of NO which are detectable with HREELS or IRAS, but not with XPS [2, 3, 32, 35]. We believe that the shift in the desorption temperature from v-NO to v_1-NO has similar reasons. The bonding mode of this molecular adsorption state, however, is unclear. In [2] and [4], discrimination of bridged, bent or linearly bound NO was based on the differences of O 1 s and N 1 s binding energies (ΔBE's) following [36]; those assignments were corroborated by HREELS results [35]. For bridged and linearly bound NO ΔBE's of 130 to 130.7 and 131 to 131.8 eV, respectively, were

found for NO on Ru(001), Ni(111) and Pt(111) [2, 4, 37] (similar results were also obtained for NO/Ir(111) [38]; for bent NO, values around 128 eV are expected [2, 36]). Further discrimination of, e.g., bridged NO bound in either two-fold or trifold sites was shown to be possible with HREELS only [35]. A ΔBE of 131.5 eV is obtained here which allows to exclude a bent species and is closer to the values expected for linearly bound NO than for bridged species. The large work function increase due to v-NO adsorption however points to a negatively charged bridged species; linearly bound NO should be positively charged and therefore decrease the work function in agreement with the results obtained for Ru(001) (see [2, 3] and references cited therein). In [11], the small decrease of $\Delta\Phi$ at saturation and the appearance of a shoulder at the high BE side of the O1s XPS maximum has been interpreted as indicative for a conversion from bridged to linearly bound NO for this coverage regime. We mention that more pronounced differences either in XPS BE's or in $\Delta\Phi$ were obtained for layers where coexistence or conversion of different bonding modes of NO could be observed unambiguously (see above). Particularly, separation of the O1s levels by 1.6 to 2.3 eV were found for bridged and linearly bound NO on Ni(111), Ru(001) and Pt(111) [2, 4, 37], whereas here merely continuous shifts of only 0.5 eV for the O1s level and 0.3 eV for the spacing between N1s and O1s are obtained when the NO coverage is increased. Similar BE changes vs. coverage are found for bridged NO on the former substrates as well and are supposed to be due to reduced backbonding in the dense layer; this could also contribute to the dip in $\Delta\Phi$. We conclude that there is no clear evidence for linearly bound NO on Ni(100), but further investigations, in particular with HREELS or IRAS, appear necessary to clarify the nature of the molecular adsorption state of NO/Ni(100) unequivocally.

Whereas the v_1-NO TPD maximum clearly stems from molecularly adsorbed NO, this cannot be concluded from our XPS data or those of [11] for the binding state giving rise to the v_2-NO desorption state at 420 K, which is strongly correlated to the β_1-N_2 maximum. It was shown in 3.2 that no molecular NO can be detected by XPS or UPS after heating to 400 K, i.e. a temperature well below the peak temperature of the v_2-NO maximum. Slight deviations of the temperature readings in both experiments, combined with the fact that stepwise heating shifts kinetic processes to lower temperatures as compared to continuous heating, may account for this discrepancy. Nevertheless, we have to allow the possibility that v_2-NO might be at least partially due to recombinative desorption. This would be in agreement with results obtained for the (100) and (110) planes of Ir [30, 31]; more careful XPS measurements and isotope exchange experiments could clear up this point. As is the case for the high temperature peaks for NO/Ir, the v_2-NO and β_1-N_2 maxima are strongly increased by preadsorbed oxygen. This would mean that the shift from v to v_1 is caused by lateral interactions within the molecular NO layer, and that during the molecular desorption, dissociation of the rest of the layer occurs part of which remains so closely correlated that some recombination occurs at slightly elevated temperature (see however [39]).

An alternative explanation for the various v-NO peaks would be analogous to that for the two closely spaced NO TPD peaks from Ru(001) [2, 3] which have been correlated with two different bonding sites, and which also could be influenced selectively by coadorbates. As mentioned, clarification would be possible best by HREELS measurements, and very careful adjustment of the temperature scales and heating modes would be desirable.

As shown, neither in this study nor in the preceding ones complete absence of all traces of impurities as desired could always be obtained. The influences of these coadsorbed species on the results obtained, however, can well be estimated from our experiments on Ni samples predosed with definite quantities of possible contaminants. These results also show that observation of decreasing oxygen coverage in PES or AES not related to desorption of oxygen should be interpreted with caution. Diffusion of the "missing" oxygen into the bulk can be safely concluded *only* if desorption of oxygen as CO or another oxygen containing compound can be definitely ruled out (see also remarks in [29]).

Acknowledgements

We thank G. Michalk and H. Schlichting for the development of microcomputer based controlling and data processing devices which were decisive for the success of the experiments and for help during

the early stages of the measurements. One of us, Shikong Shen, thanks the Alexander von Humboldt Foundation for a fellowship. This work has been supported by the Deutsche Forschungsgemeinschaft through Sonderforschungsbereich 128.

[1] R. I. Masel, E. Umbach, J. C. Fuggle, and D. Menzel, Surface Sci. **79,** 26 (1979).
[2] E. Umbach, S. Kulkarni, P. Feulner, and D. Menzel, Surface Sci. **88,** 65 (1979).
[3] P. Feulner, S. Kulkarni, E. Umbach, and D. Menzel, Surface Sci. **99,** 489 (1980).
[4] M. J. Breitschafter, E. Umbach, and D. Menzel, Surface Sci. **109,** 493 (1981).
[5] K. K. Pandey, Coordination Chemistry Reviews **51,** 69 (1983).
[6] J. H. Enemark and R. D. Felthaus, Coordination Chemistry Reviews **13,** 339 (1974). – A. F. Wells, Structural Inorganic Chemistry, 3rd ed. Oxford University Press 1962. – F. A. Cotton and G. Wilkinson, Advanced Inorganic Chemistry, 4th ed. Wiley, New York 1980, p. 91.
[7] A. Schichl and N. Rösch, Surface Sci. **137,** 261 (1984). G. Doyen and G. Ertl, Surface Sci. **69,** 157 (1977). – I. P. Batra and C. R. Brundle, Surface Sci. **57,** 12 (1976).
[8] M. Onchi and H. E. Farnsworth, Surface Sci. **13,** 425 (1969).
[9] Y. Sakisaka, M. Miyamura, J. Tamaki, M. Nishijima, and M. Onchi, Surface Sci. **93,** 327 (1980).
[10] G. L. Price and B. G. Baker, Surface Sci. **91,** 571 (1980).
[11] D. E. Peebles, E. L. Hardegree, and J. M. White, Surface Sci. **148,** 653 (1984).
[12] J. Stöhr and R. Jaeger, Phys. Rev. **B 26,** 4111 (1982).
[13] H. A. Engelhardt, P. Feulner, H. Pfnür, and D. Menzel, J. Phys. **E 10,** 1133 (1977).
[14] P. Feulner and D. Menzel, J. Vac. Sci. Technol. **17,** 662 (1980).
[15] P. R. Norton, R. L. Tapping, and J. W. Goodale, Surface Sci. **65,** 13 (1977). – G. Greiner and D. Menzel, J. Catalysis **77,** 382 (1982). – G. Greiner, Ph.D. thesis, Technische Universität München 1980.
[16] M. J. Breitschafter, Diplom thesis, Technische Universität München 1980.
[17] D. Menzel and J. C. Fuggle, Surface Sci. **74,** 403 (1978).
[18] I. P. Batra and C. R. Brundle, Surface Sci. **57,** 12 (1976). – C. R. Brundle, J. Vacuum Sci. Technol. **13,** 301 (1976).
[19] J. H. Scofield, J. El. Spectr. **8,** 129 (1976).
[20] E. Umbach, Surface Sci. **117,** 482 (1982).
[21] W. E. Moddeman, T. A. Carlson, M. O. Krause, B. P. Pullen, W. E. Bull, and G. K. Schweitzer, J. Chem. Phys. **55,** 2317 (1971). – J. C. Fuggle, E. Umbach, R. Kakoschke, and D. Menzel, J. Electron. Spectr. **26,** 111 (1982).
[22] J. Topping, Proc. Roy. Soc. London **A 114,** 67 (1924). J. D. McDonald and C. A. Barlow, J. Chem. Phys. **39,** 412 (1963).
[23] B. E. Koel, D. E. Peebles, and J. M. White, Surface Sci. **125,** 709 (1983).
[24] K. Akimoto, Y. Sakisaka, M. Nishijima, and M. Onchi, Surface Sci. **82,** 349 (1979).
[25] R. J. Gorte and L. D. Schmidt, Surface Sci. **109,** 367 (1981).
[26] R. Treichler and D. Menzel, unpublished results.
[27] J. L. Falconer and R. J. Madix, Surface Sci. **48,** 393 (1975).
[28] H. Schlichting, diploma thesis, Technische Universität München 1981.
[29] G. L. Price, B. A. Sexton, and B. G. Baker, Surface Sci. **60,** 506 (1976).
[30] J. Küppers and H. Michel, Surface Sci. **85,** L 201 (1979).
[31] D. E. Ibbotson, T. S. Wittrig, and W. H. Weinberg, Surface Sci. **110,** 294 (1981).
[32] J. L. Gland and B. A. Sexton, Surface Sci. **94,** 355 (1980).
[33] Pin Ho and J. M. White, Surface Sci. **137,** 103 (1984).
[34] Handbook of Chemistry and Physics, 53rd ed. CRC Press 1972, p. F 183.
[35] H. Conrad, R. Scala, W. Stenzel, and R. Unwin, Surface Sci. **145,** 1 (1984). – P. A. Thiel, W. H. Weinberg, and J. T. Yates, Jr., Chem. Phys. Lett. **67,** 403 (1979).
[36] C. C. Su and J. W. Faller, J. Organomet. Chem. **84,** 53 (1975).
[37] M. Kiskinova, G. Pirug, and H. P. Bonzel, Surface Sci. **150,** 285 (1984).
[38] P. A. Zhdan, G. K. Boreskov, A. I. Bronin, and A. P. Schepelin, J. Catalysis **60,** 93 (1979).
[39] In view of the change of the ν_1/ν_2 peak height ratio with decreasing oxygen contamination (from 2.3 to 1 (Fig. 7) to 4.3 to 1 (Fig. 10) at saturation), one has to raise the question if the remaining ν_2-state shown in Fig. 8 might still be due to oxygen impurities on the surface. We do not believe this; as indicated above, the absence of preadsorbed oxygen was carefully checked with AES for the TPD measurements. The missing of NO desorption from layers of O dosed on Ni(100) precovered with atomic nitrogen (Fig. 11) does not rule out the interpretation given above. ν_2-NO could form from N concentrations exceeding the saturation coverage of the β_2-N_2 state and giving rise to the desorption peak obtained for the pure N-layer at 370 K (see Figure 11).